of the minima in all SiC polytypes, they may at the same time determine the indirect energy gaps, which must depend on both the position and the strength of the discontinuities. Hence it may be possible to correlate the energy gaps with x-ray data or with calculated structure factors. It is not obvious that there should be a correlation of gap with "percent hexagonal" as shown in Fig. 3 of Ref. 10.

The consequences for transport properties are also of interest. The conduction-band minima are expected to depend on polytype, but the valence-band maxima are not, since they occur at $\mathbf{k}=0$. Hence, n-type samples of various polytypes are expected to have diverse transport properties, but not p-type samples.

ACKNOWLEDGMENTS

We wish to thank N. R. Anderson and M. M. Sopira, Jr. for technical assistance.

PHYSICAL REVIEW VOLUME 137, NUMBER 5A 1 MARCH 1965

Paramagnetic Resonance Study of a Deep Donor in Silicon

G. W. LUDWIG
General Electric Research Laboratory, Schenectady, New York
(Received 6 October 1964)

The impurity sulfur acts as a double donor in silicon. Assuming the ion to be substitutional, S^+ is analogous to neutral phosphorus, except that the binding energy of the donor electron is much greater. Here we report paramagnetic resonance absorption of S^+, including a detailed study, made using electron-nuclear-double-resonance techniques, of the hyperfine interaction with neighboring Si^{29} nuclei. We find hyperfine interaction constants which are inconsistent with the Kohn-Luttinger wave function (derived from the effective-mass approximation and intended for shallow donors) as applied to S^+. This result indicates that contributions to the S^+ donor wave function from parts of the silicon energy band structure (notably $\Delta_{2'}$) other than the Δ_1 conduction-band minima are important. Resonant absorption also is reported for other centers including a sulfur pair and several iron-sulfur pairs.

I. INTRODUCTION

MANY elements can be introduced into silicon in sufficient concentration that electrical properties are significantly affected. Examples are the Column III elements B, Al, and Ga (shallow acceptor impurities); the Column V elements P, As, and Sb (shallow donors); the Column VI element S, and transition metals of the 3d group. Electronic properties of the shallow-level impurities have been interpreted in terms of an effective mass treatment by Kohn and Luttinger. In the case of the shallow donors, they find an approximate wave function for the donor electron of the form[1]

$$\Psi(\mathbf{r})=\sum_{j=1}^{6}\alpha_j F_j(\mathbf{r})u_j(\mathbf{r})\exp(i\mathbf{k}_j{}^0\cdot\mathbf{r}). \quad (1)$$

Here, $u_j(\mathbf{r})\exp(i\mathbf{k}_j\cdot\mathbf{r})$ is the Bloch function at the jth minimum of the Δ_1 conduction band, $F_j(\mathbf{r})$ is a hydrogen-like envelope function, and the complete wave function is obtained by summing contributions from each of six minima of the Δ_1 band, located at points such as $(0,0,k_0)$ in reciprocal space. The Kohn-Luttinger treatment accounts for the binding energy of the donor electron in order of magnitude, for the positions of excited states, as determined optically, and for interference effects in the donor wave function found experimentally by Feher by paramagnetic resonance techniques.[2]

The electronic structure of deep-level defects in silicon (and other semiconductors) is less well known, although progress has been made in a number of cases.[3–6]

From the standpoint of a comparison with the shallow donor impurities (and the Kohn-Luttinger treatment), perhaps the most interesting of the deep-level impurities is the element sulfur. In the third row of the Periodic Table silicon, phosphorus, and sulfur are the Column IV, V, and VI elements, respectively. The electrical properties of sulfur in silicon have been studied by Carlson *et al.*,[7] who report that it is a double donor. There appears to be no definitive evidence that sulfur impurities in silicon occupy substitutional rather than

[1] W. Kohn and J. M. Luttinger, Phys. Rev. **97**, 883 (1955); **98**, 915 (1955); Solid State Phys. **5**, 257 (1957).

[2] G. Feher, Phys. Rev. **114**, 1219 (1959).

[3] Paramagnetic resonance has been used as an experimental tool for obtaining detailed information about the electronic structure of a number of paramagnetic deep level impurities. See, for example, the studies of radiation damage defects in silicon by Watkins and collaborators (Ref. 4), of transition metal ions in silicon by Ludwig and Woodbury (Ref. 5), and of nitrogen in diamond by Smith *et al.* (Ref. 6).

[4] G. W. Watkins and J. W. Corbett, Discussions Faraday Soc. **31**, 86 (1961).

[5] G. W. Ludwig and H. H. Woodbury, Solid State Phys. **13**, 223 (1962).

[6] W. V. Smith, P. P. Sorokin, I. L. Gelles, and G. J. Lasher, Phys. Rev. **115**, 1546 (1959).

[7] R. O. Carlson, R. N. Hall, and E. M. Pell, Phys. Chem. Solids **8**, 81 (1959).

interstitial sites. If, in fact, they are substitutional, the donor electron of S^+ experiences an environment which is very similar to that experienced by the donor electron of phosphorus except for an extra unit of nuclear charge. (Similarly, phosphorus is the simplest shallow donor to treat theoretically because its ion core is identical to that of silicon except for its extra nuclear charge.)

In this paper, we report a study of sulfur impurities in silicon using paramagnetic resonance techniques. Resonant absorption is reported for S^+. As expected on a substitutional model, S^+ has an electron spin of $\frac{1}{2}$ (there is one unpaired electron, the donor electron). The isotropy of the g tensor and of the hyperfine interaction with S^{33} indicate that the S^+ ion is isolated in the lattice rather than having nearby charge compensation.

The hyperfine interaction of the donor electron with Si^{29} nuclei of the host lattice was of particular interest to the present study. The reason for this is that the wave function amplitude of the donor electron at a lattice site can be deduced from the contact part of this interaction. An object of the study was to compare an experimentally determined set of wave function amplitudes with a theoretical set obtained using the Kohn-Luttinger treatment.

Using the electron-nuclear double resonance (ENDOR) technique of Feher, the hyperfine interaction was measured for Si^{29} occupying eight sets of neighboring sites to the sulfur ion. The information obtained from experiment consisted of both the principal axes and the principal values of the interaction. From the principal axes the symmetry of the arrangement of neighbors relative to the sulfur ion was deduced. Unfortunately, even with the help of the Kohn-Luttinger treatment, it was not possible to assign a given hyperfine coupling unambiguously to a particular set of neighbors (e.g., to neighbors occupying 333 rather than 444 sites). It was not even possible to conclude with certainty that the S^+ occupies substitutional sites rather than the particular interstitial sites which have a similar arrangement of neighbors.

A comparison of the experimental results with the Kohn-Luttinger treatment makes it clear that the treatment in its simple form breaks down in the case of S^+, whether S^+ be substitutional or interstitial. Ham has suggested that the disagreement with experiment may, in part, reflect a contribution to the wave function from the $\Delta_{2'}$ conduction band.[8] He points out that the separation of this band is comparable to the binding energy of the donor, and a contribution of proper phase could account for certain inconsistencies between theory and experiment.

No resonant absorption was detected for S^{2+} and S^0 in silicon; presumably these ions contain no unpaired electrons.

In the course of studying sulfur impurities in silicon by paramagnetic resonance techniques, we have found that sulfur impurities tend to pair with each other, as well as with iron impurities in the crystal. The spectra of these pairs were also studied, although in lesser detail.

Experimental techniques are discussed in Sec. II, while III is devoted to a description of the resonance spectrum. The determination of the hyperfine coupling with Si^{29} and the comparison with the Kohn-Luttinger treatment are treated in IV. Spectra of other centers are dealt with in V.

II. EXPERIMENTAL TECHNIQUES

Samples of silicon containing sulfur were prepared in the following manner[9]: Bars were cut from single-crystal silicon containing phosphorus (a shallow donor), boron (a shallow acceptor), or no intentionally added impurities. Typically, the bars were $3.5\times3.5\times15$ mm^3 in dimension and had their long axis along a [110] direction. The bars were sealed into quartz ampoules containing several milligrams of sulfur and were maintained overnight at $\approx$1300°C. The bars were removed from the ampoules, were reheated to 1300°C for several minutes, and finally were quenched by blowing them directly from the furnace into a beaker of ethylene glycol.

Samples were mounted in a cylindrical $TE011$ mode cavity with a [110] axis vertical, and examined in a paramagnetic resonance spectrometer which operates at about 14 kMc/sec. The magnetic field can be rotated about a vertical axis, and spectra were obtained for H in the (110) plane.

Spectra were also taken with the samples subjected to uniaxial stress. The experimental procedure was to glue the sample between two phosphor-bronze rods using a jig to hold the rods coaxial with the sample. The assembly then was mounted so that one rod extended through an axial hole in the top of the cylindrical cavity. Stress was transmitted to the assembly by a stainless steel rod, which was confined within a stainless steel tube coaxial with the cavity.

In ENDOR, one is concerned with transitions in which a nucleus reorients while the electron spin remains fixed ($\Delta M=0$, $\Delta m=\pm1$). To study such transitions experimentally, the sample was cooled to a temperature in the liquid-helium range (1.35–4.3°K), where the spin-lattice relaxation time of the S^+ center becomes quite long. The spectrometer was tuned to the dispersion signal, and the dc magnetic field was modulated over a portion of the appropriate paramagnetic resonance line. The sample was also exposed to an rf magnetic field by driving a specially designed cylindrical cavity,[9] constructed in the form of a helix, with a rf generator. The frequency of the rf generator was varied slowly using a motor drive, and ENDOR transitions were detected via the associated change in amplitude

[8] F. S. Ham (private communication).

[9] For additional experimental details see G. W. Ludwig and H. H. Woodbury, Phys. Rev. **113**, 1014 (1959); H. H. Woodbury and G. W. Ludwig, *ibid.* **117**, 102 (1960).

of the paramagnetic resonance signal. The strongest ENDOR lines[10] were obtained at 1.35°K with the sample exposed to light, from a tungsten bulb, to reduce the electron spin relaxation time.

The sample cavity in most paramagnetic resonance spectrometers terminates one arm of a magic tee bridge, while the "fourth arm" of the bridge is terminated by a matched load. The sensitivity of such spectrometers when operated in the dispersion mode often is limited by noise arising from frequency instability of the microwave source. We have obtained improved signal-to-noise ratios by replacing the matched load with a resonant cavity matched in frequency, quality factor, and coupling coefficient to the sample cavity, as suggested by Redhardt and by others.[11] The frequency is tuned by changing the length of the cavity; the Q is adjusted by moving a piece of low resistivity silicon into or out of the cavity; and the coupling coefficient is controlled by a screw in the coupling iris. Such a dummy cavity makes the microwave bridge insensitive to frequency instability of the source. The resulting increase in the signal-to-noise ratio was important in obtaining the ENDOR data.

III. PARAMAGNETIC RESONANCE SPECTRUM

The spectra observed in sulfur-doped silicon crystals depended upon the impurity content of the starting material, upon the freshness of the sample, and in addition showed some uncontrolled variation. Usually, a substantial amount of iron, not detected in the starting material, was found in the samples. The spectrum which we attribute to S^+ is isotropic and has a $g\simeq 2$. It was detected only if p-type starting material was used, the maximum intensity being obtained with material containing $\sim 3\times 10^{16}$ B/cm^3, part of which served to compensate iron impurities. Presumably one requires p-type starting material to soak up electrons donated by the sulfur in forming S^+. With concentrations of boron larger than 3×10^{16}/cm^3, the intensity of the resonance signal tended to decrease, presumably because of formation of S^{2+}. However, the signal intensity could then be enhanced by exposing the sample to light from a tungsten bulb while the sample was thermostated in the spectrometer at low temperature. A likely explanation is that S^+ was generated when electrons liberated by the light were trapped by S^{2+} ions.

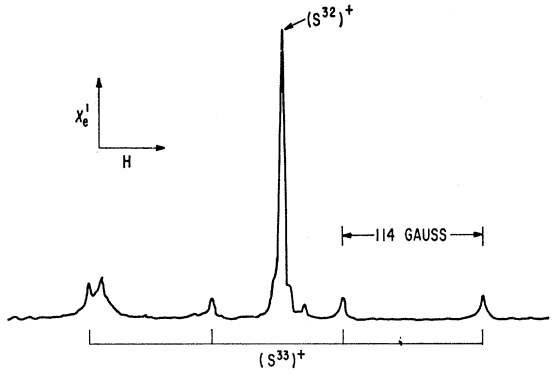

FIG. 1. Spectrum of S^+ under rapid passage conditions in a sample enriched to contain 26% S^{33}. The almost equally spaced satellite lines are about 9% as intense as the main line, which is consistent with the above enrichment if the resonant center contains one sulfur nucleus. The two other weak lines are associated with small amounts of Fe^0 and Cr^+ present in the sample.

The S^+ spactrum has been observed at 77°K in samples having a sufficiently low conductivity. It consists of one main line plus some weaker structure. In order to obtain additional evidence as to whether the spectrum is associated with sulfur, samples were prepared containing[12] sulfur enriched to 26% in the isotope S^{33}, which has a nuclear spin $I=\frac{3}{2}$. As shown in Fig. 1, one then finds four well-resolved satellite lines. The appearance of $2I+1$ satellites of the proper intensity relative to the main line is strong evidence that the resonance center involves one and only one sulfur ion.

The spin Hamiltonian of S^+ is

$$\mathcal{H}=g\beta\mathbf{S}\cdot\mathbf{H}+A\mathbf{S}\cdot\mathbf{I}-\gamma\beta_N\mathbf{H}\cdot\mathbf{I}+\sum_k(\mathbf{S}\cdot T_k\cdot\mathbf{I}_k-\gamma_k\beta_N\mathbf{H}\cdot\mathbf{I}). \quad (2)$$

In (2), the first three terms describe the Zeeman interaction of the electron spin $\mathbf{S}$ and its hyperfine coupling with S^{33}, while the remaining terms take into account the hyperfine coupling with Si^{29} nuclei of the host lattice. Omitting the Si^{29} terms, the $(M-1, m)$ to (M,m) resonance transition is given by

$$h\nu=g\beta H+Am+[I(I+1)-m+m(2M-1)]A^2/2g\beta H. \quad (3)$$

From the spectrum of Fig. 1, we find

$$g=2.0054\pm 0.0002,\qquad |A|=(104.2\pm 0.2)\times 10^{-4}\ \text{cm}^{-1}. \quad (4)$$

One cannot immediately conclude from the lack of fine structure on the main line in Fig. 1 that the electron spin of the S^+ center is $\frac{1}{2}$. The isotropy of the g tensor and of the tensor describing the hyperfine interaction with S^{33} is evidence that the S^+ ion occupies a site of high symmetry. The symmetry of the hyperfine interaction with Si^{29}, described in Sec. IV, shows that the site in fact has tetrahedral symmetry, so that one expects no fine structure splitting of the S^{32} line for $S\leqslant\frac{3}{2}$. However, it is possible to deduce the value of S by measuring the frequency of the S^{33} ENDOR transitions. To second order in the hyperfine interaction

[10] ENDOR mechanisms have been discussed by Lambe *et al.* [Phys. Rev. **122**, 1161 (1961)].

[11] E. Redhardt, Z. Angew. Phys. **13**, 108 (1961); A. F. Mehlkopf and J. Smidt, Rev. Sci. Instr. **32**, 1421 (1961).

[12] The sulfur enriched in S^{33} was obtained from the Isotope Sales Department, Oak Ridge National Laboratory, Oak Ridge, Tennessee.

parameter A, the frequency f of the transition between the states (M,m) and $(M, m-1)$ is given by

$$hf=|AM-\gamma\beta_N H -[S(S+1)+(2m-1)M-M^2]A^2/2g\beta H|. \quad (5)$$

ENDOR data was obtained with the spectrometer tuned to the second highest S^{33} hyperfine line of Fig. 1 at $\nu=13885$ Mc/sec and $H=4998$ G. The data is summarized in Table I along with the ENDOR frequencies predicted from (5) for that ν and H, and taking $|A|=104.2\times10^{-4}$ cm^{-1} and $\gamma=\mu/I=+0.428$ for S^{33}. Despite the fact that three rather than the expected four ENDOR transitions were detected, an inspection of Table I indicates that $S=\frac{1}{2}$. In confirmation of this value, no fine structure, owing to the term $m(2M-1)A^2/2g\beta H$ in (3), is found on the S^{33} hyperfine lines, although structure would be expected for $S>\frac{1}{2}$. In addition, no fine structure was observed when the sample was exposed to a compressive uniaxial stress ≈3000 kg/cm^2 in a [110] direction, which lowers the symmetry of the S^+ site.

The paramagnetic resonance spectrum of S^+ is qualitatively similar to that of P^0. In both cases, the resonant center is a single impurity ion, as shown by the hyperfine interaction with the central nucleus, and the resonant absorption is associated with a single unpaired electron ($S=\frac{1}{2}$). The isotropy of the g tensor and of the hyperfine interaction with the central nucleus is an indication that the ion occupies a site of tetrahedral symmetry and is unassociated with other defects. The g factor is close to the free-electron value, consistent with the view that the ground state of the ion is orbitally nondegenerate.

In the absence of a detailed model of the S^+ center, however, it is not possible to conclude from the paramagnetic resonance spectrum that the S^+ ion, like P^0, is substitutional; both substitutional sites and the interstitial sites of maximum symmetry in the silicon lattice have tetrahedral symmetry, and somewhat similar arrangements of near silicon neighbors. In an effort to obtain evidence as to which site is occupied by the S^+ ion, samples containing S^+ were bombarded with electrons of energy sufficient to produce lattice vacancies. If the S^+ ions were interstitial, a fraction of them might trap vacancies to become substitutional.[13] Were the ions substitutional, they might trap vacancies to form centers analogous to the E center formed by phosphorus ions.[14] However, no new spectra were found.

TABLE I. ENDOR transitions of $(S^{33})^+$.

Transition[a]	f_{meas} (Mc/sec)	f_{calc} (Mc/sec) $S=\frac{1}{2}$	f_{calc} (Mc/sec) $S=\frac{3}{2}$
$(\pm\frac{1}{2},\pm\frac{1}{2})$ to $(\pm\frac{1}{2},\mp\frac{1}{2})$	152.8	152.9	142.4
$(\pm\frac{1}{2},\mp\frac{1}{2})$ to $(\pm\frac{1}{2},\mp\frac{3}{2})$	156.3	156.4	145.9
$(\mp\frac{1}{2},\pm\frac{1}{2})$ to $(\mp\frac{1}{2},\mp\frac{1}{2})$	159.5	159.7	170.2
$(\mp\frac{1}{2},\mp\frac{1}{2})$ to $(\mp\frac{1}{2},\mp\frac{3}{2})$		163.2	173.7

[a] The upper and lower signs apply to $A>0$ and $A<0$, respectively.

IV. HYPERFINE INTERACTION WITH Si^{29}

The hyperfine interaction of the donor electron with the 4.7% abundant isotope Si^{29} occupying a nearby lattice site may be divided into two parts: the contact or Fermi-Segre interaction and the dipolar interaction. The contact interaction has the form

$$\mathcal{H}_c=(8\pi/3)g\beta\gamma_k\beta_N|\Psi(r_k)|^2\mathbf{S}\cdot\mathbf{I}_k. \quad (6)$$

The coefficient of $\mathbf{S}\cdot\mathbf{I}_k$ in (6) represents an isotropic contribution to the hyperfine interaction tensor T_k defined by (2); from it one can deduce $|\Psi(r_k)|^2$, the square of the amplitude of the donor wave function at the kth lattice site. As Feher has pointed out, the values of $|\Psi(r_k)|^2$ for a number of lattice sites constitute a map of the donor wave function.

The dipolar interaction between an electron at $\mathbf{r}$ and Si^{29} nucleus at $\mathbf{r}_k$ has the form

$$\mathcal{H}_D=-g\beta\gamma\beta_N(r-r_k)^{-3} \times\{\mathbf{S}\cdot\mathbf{I}-3[\mathbf{I}_k\cdot(\mathbf{r}-\mathbf{r}_k)][\mathbf{S}\cdot(\mathbf{r}-\mathbf{r}_k)]/(r-r_k)^2\}. \quad (7)$$

When (7) is averaged over the donor wave function one obtains both an isotropic and an anisotropic contribution to the hyperfine tensor. The isotropic contribution is expected to be small compared to that from the contact interaction. The anisotropic contribution provides additional information about the donor wave function; however, it has not been satisfactorily accounted for even for the shallow donors. One can, however, use the symmetry of the anisotropic contribution as an aid in identifying the lattice site $\mathbf{r}_k$ to which a particular hyperfine tensor belongs.

The remainder of IV is divided into several parts: In A, we describe the structure of the silicon lattice and the symmetry of the hyperfine interaction tensor for various neighbors to a substitutional site and to the interstitial site of similar symmetry; B deals with the experimental determination of the hyperfine interaction of the donor electron with Si^{29}; in C the Kohn-Luttinger treatment is applied to S^+; and in D the experimentally determined parameters are discussed in light of the Kohn-Luttinger treatment.

A. Neighbors to Substitutional and Interstitial Sites

Silicon crystallizes in the diamond lattice in which each substitutional atom is surrounded by four nearest neighbors in a tetrahedral arrangement (see Fig. 2).

[13] Such trapping has been reported in the case of interstitial transition metal ions in silicon. See H. H. Woodbury and G. W. Ludwig, Phys. Rev. Letters **5**, 537 (1960).

[14] See G. D. Watkins and J. W. Corbett, Phys. Rev. **134**, A1359 (1964).

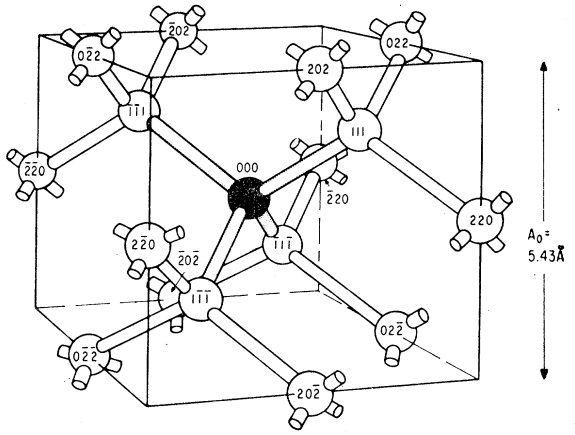

FIG. 2. The silicon lattice showing the nearest and second-nearest neighbors to a substitutional site.

The successive shells of near neighbors to a substitutional site and some of their characteristics are listed in Table II, while similar information for an interstitial site is given in Table III. We may note that in both cases every neighbor falls into one of four classes which can readily be distinguished by the symmetry of the hyperfine coupling with the donor electron. The classes are as follows:

(a) The 111 class of neighbors (for example, the neighbors at 333, $\bar{3}\bar{3}3$, $3\bar{3}\bar{3}$, and $\bar{3}3\bar{3}$). The four neighbors in a shell are arranged at the corners of a tetrahedron, each neighbor being located in a [111] direction from the central site. Thus each neighbor lies on an axis of threefold rotation symmetry, and the principal axes of its hyperfine interaction tensor are the [111] axis and any two mutually perpendicular directions in the (111) plane. The tensor has principal values $T_1 = T_{\parallel}$, and $T_2 = T_3 = T_{\perp}$, where $T_{\parallel}$ refers to the value along the [111] axis. For H in a low-symmetry direction in a

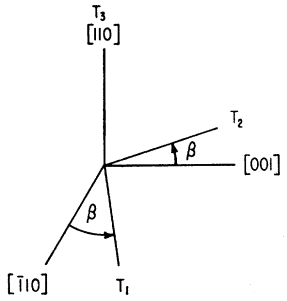

FIG. 3. The principal axes of the hyperfine tensor for a Si^{29} atom belonging to the 110 class of neighbors. With T replaced by g, the figure shows the principal axes of the g tensor for a center having a (110) plane of reflection symmetry (Sec. V.B).

(110) plane, the complete hyperfine (or ENDOR) pattern consists of three sets of lines, which may or may not be resolved, representing 1, 1, and 2 neighbors, respectively.

(b) The 100 class of neighbors. There are six neighbors in a shell, each located on a cubic crystalline axis passing through the central site. Each neighbor also lies in two (110) planes of reflection symmetry, and the principal axes of the hyperfine interaction tensor are the cubic axis (the axis of T_1) and the two [110] directions perpendicular to the reflection planes (the axes of T_2 and T_3). For H in a (110) plane, there are four sets of hyperfine lines representing 1, 1, 2, and 2 neighbors.

(c) The 110 class of neighbors. There are twelve neighbors in a shell, each of which is located in a (110) plane of reflection symmetry passing through the central ion. One principal axis of the hyperfine interaction tensor, that of T_3, is the perpendicular to the reflection plane; the other two lie within this plane. We choose the axis of T_1 such that $T_1 > T_2$. As shown in Fig. 3, the angle between the axis of T_1 and the [$\bar{1}$10] axis within the (110) plane must also be specified in defining T. For H in a (110) plane the hyperfine pattern consists of 2 sets of lines representing 1 neighbor each and 5 sets of lines representing 2 neighbors each.

TABLE II. Near neighbors to a substitutional site.

Shell	Neighbor[a]	Number of sites	Distance (Å)
1	111	4	2.35
2	220	12	3.8
3	311	12	4.5
4	400	6	5.4
5	331	12	5.9
6	$(422)_a$	12	6.6
	$(422)_b$	12	6.6
7	511	12	7.1
	333	4	7.1
8	440	12	7.7
9	531	24	8.0
10	620	24	8.6
11	533	12	8.9
12	$(444)_a$	4	9.4
	$(444)_b$	4	9.4
13	711	12	9.7
	551	12	9.7

[a] Neighbors are labeled taking the substitutional site as the origin.

TABLE III. Near neighbors to an interstitial site.

Shell	Neighbor[a]	Number of equivalent sites	Distance (Å)
1	111	4	2.35
2	200	6	2.7
3	311	12	4.5
4	$(222)_a$	4	4.7
	$(222)_b$	4	4.7
5	331	12	5.9
6	420	24	6.1
7	511	12	7.1
	333	4	7.1
8	531	24	8.0
9	$(442)_a$	12	8.1
	$(442)_b$	12	8.1
	600	6	8.1
10	$(533)_a$	12	8.9
	$(533)_b$	12	8.9
11	$(622)_a$	12	9.0
	$(622)_b$	12	9.0

[a] Neighbors are labeled taking the interstitial site as the origin.

(d) The low-symmetry class of neighbors. For sites such as 531 there are 24 neighbors in a shell located at low symmetry points. Using symmetry alone, one cannot predict the principal axes of T. For H in a (110) plane, the hyperfine pattern consists of 21 sets of lines each representing 2 neighbors.

If one makes a detailed comparison of the hyperfine patterns to be expected from neighbors belonging to the above four classes it becomes clear that assignment of a given hyperfine pattern to neighbors of a given class will be unambiguous, provided the experimental data is sufficiently complete. On the other hand, from symmetry arguments alone one cannot distinguish between different sets of neighbors belonging to the same class. Thus one may be able to say with assurance that a given hyperfine pattern belongs to neighbors having 110 symmetry, but other arguments are necessary for deciding whether one is dealing with 220 or 311 or 331 neighbors.

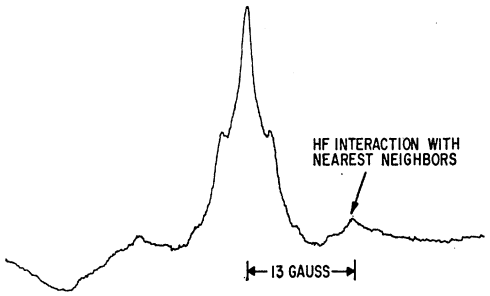

FIG. 4. The structure of the S^+ line (dispersion derivative). The dip on the left is the resonance of sulfur pairs (see Sec. V.A) viewed under rapid passage conditions.

B. Experimental Determination of the Hyperfine Coupling

In determining the hyperfine coupling with Si^{29}, the $\Delta M=\pm 1$, $\Delta m=0$ paramagnetic resonance transitions were used to study resolved hyperfine lines. The ENDOR technique was then employed to study partially resolved or unresolved structure.

A slow scan over the S^+ line for H in a cubic direction is shown in Fig. 4. In addition to the main line, which shows partially resolved structure, there are two weak satellites which are symmetrically placed and have the same shape as the main line. The hyperfine interaction tensor describing the satellite pattern was successfully determined although the satellite structure is incompletely resolved for most directions of H. The structure is associated with neighbors having 111 symmetry.

From the Kohn-Luttinger type of analysis to be described in C, it was anticipated that, assuming S^+ to be substitutional, the hyperfine coupling with 400 neighbors would be as strong or stronger than that with any other neighbors. Therefore, the S^+ spectrum was searched at high gain for other satellite structure with H in the [001] and other important crystallographic directions. None was found.

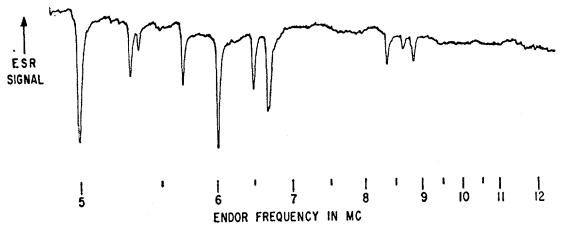

FIG. 5. ENDOR transitions at $\approx 1.35°$K of Si^{29} neighbors to a S^+ site for H in a [001] direction (Ref. 10).

In electron-nuclear double resonance one induces transitions described by $\Delta M=0$, $\Delta m_j=\pm 1$, $\Delta m_k=0$ for $j\neq k$. With hyperfine terms having the form (2) the Si^{29} ENDOR frequencies f are given approximately by[15]

$$hf=[\sum_{i=1}^{3}(T_{ij}M-\gamma_j\beta_N H)^2\cos^2\theta_{ij}]^{1/2}. \quad (8)$$

Here $M=\pm\frac{1}{2}$, and the θ_{ij} are the angles between the direction of the magnetic field and the ith principal axis of the hyperfine tensor for Si^{29} at the jth lattice site.

A portion of the Si^{29} ENDOR spectrum for the magnetic field in a cubic direction is shown in Fig. 5. It consists of 10 lines between 5 and 9 Mc/sec, one of which is a doublet. When the magnetic field is rotated to a lower symmetry direction in the (110) plane, each of the lines splits. When necessary, the resulting spectrum was studied by taking measurements every 5° within this plane using a slower scan so as to obtain increased resolution. Equation (8) was then used to analyze the ENDOR lines in terms of the hyperfine interaction with seven different sets of neighbors. As examples the angular dependence of the ENDOR spectra of two sets of neighbors are shown in Figs. 6 and 7.

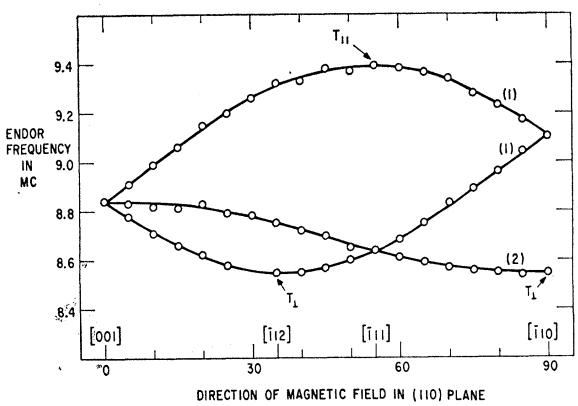

FIG. 6. Angular dependence of the ENDOR transitions of a group of Si^{29} neighbors having 111 symmetry. The relative intensities of the transitions are as indicated.

[15] See, for example, the Appendix in H. H. Woodbury and G. W. Ludwig, Phys. Rev. 124, 1083 (1961).

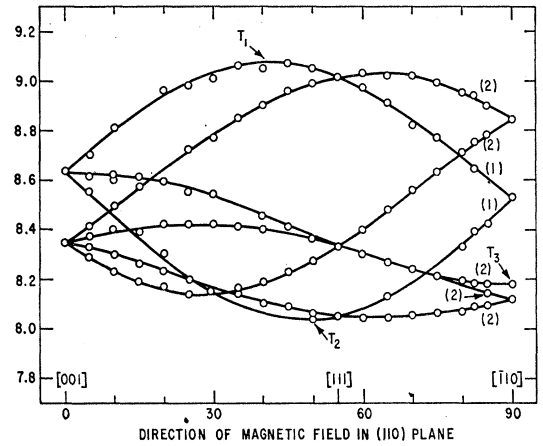

FIG. 7. Angular dependence of the ENDOR transitions of a group of Si^{29} neighbors having 110 symmetry. The relative intensities of the transitions are as indicated.

When the magnetic field was adjusted to one side of the S^+ line it was also possible to detect ENDOR transitions in the range 14–33 Mc/sec corresponding to the satellite structure shown in Fig. 4. The hyperfine interaction constants determined by ENDOR agreed with those obtained previously by direct measurements of the hyperfine splitting.

A careful search was made for additional ENDOR transitions in the range 8–18 Mc/sec, under conditions where both the high-frequency ENDOR transitions and the low-frequency transitions of Fig. 5 could be detected. None was located. One would expect still higher frequency ENDOR transitions to result in resolved structure on the resonance line; it is thus felt that all hyperfine interactions $T_j > 0.42\times10^{-4}$ cm^{-1} have been detected and studied. A search was also made for ENDOR transitions corresponding to weaker interactions. A number of overlapping transitions were found but were not successfully analyzed.

In all cases T_1, T_2, and T_3 were found experimentally to have the same sign, and it was assumed that all are negative, since γ_k is negative [see (6)].

The resulting parameters describing the hyperfine coupling with Si^{29} at 8 different lattice sites are summarized in Table IV.

C. Application of the Kohn-Luttinger Treatment to S^+

Kohn and Luttinger find that the wave function of a shallow donor electron is given approximately by

$$\Psi(\mathbf{r})=\sum_{j=1}^{6}\alpha_j F_j(\mathbf{r})u_j(\mathbf{r})\exp(i\mathbf{k}_j^0\cdot\mathbf{r}). \quad (9)$$

Here $u_j(\mathbf{r})\exp(i\mathbf{k}_j^0\cdot\mathbf{r})$ is the Bloch function at the jth minimum of the conduction band and $F_j(\mathbf{r})$ is a hydrogen-like envelope function. The wave function is constructed from contributions from each of the six equivalent minima, located at points such as $(0,0,k_0)$. Each $F(\mathbf{r})$ is the solution of an effective-mass equation of the form

$$\left[\frac{h^2}{2m_t}\left(\frac{\partial^2}{\partial x^2}+\frac{\partial^2}{\partial y^2}\right)+\frac{h^2}{2m_l}\frac{\partial^2}{\partial z^2}-U(\mathbf{r})+E\right]F_z(\mathbf{r})=0. \quad (10)$$

In (10), m_t and m_l are transverse and longitudinal effective masses, while $U(\mathbf{r})$ is the impurity potential.

As discussed by Kohn and Luttinger,[1] an approximate $F_z(\mathbf{r})$ is obtained by taking $U(r)=-e^2/\kappa r$ in (10) and substituting for $F_z(\mathbf{r})$ the expression

$$F_z(\mathbf{r})=(\pi a^2 b)^{-1/2}\exp\{-[(x^2+y^2)/a^2+z^2/b^2]^{1/2}\}. \quad (11)$$

Here a and b are parameters which are varied to minimize the energy. For silicon they find $a=25.0$ Å and $b=14.2$ Å, the large anisotropy in the radius of the envelope function being a consequence of the large effective-mass ratio. The corresponding effective mass value of the binding energy ($E_{\text{eff mass}}$) is 0.029 eV.

Actually, within the central cell the expression $U(r)=-e^2/\kappa r$ is a poor approximation to the impurity potential, and donor binding energies tend to be somewhat larger than the effective-mass value of 0.029 eV. An $F_z(\mathbf{r})$ which retains the form (11) but which is more accurate for large $\mathbf{r}$ is obtained by replacing a and b in (11) with na and nb, where

$$n=(E_{\text{eff mass}}/E_{\text{obs}})^{1/2} \quad (12)$$

and E_{obs} is the observed binding energy of the donor.

A still different and presumably better $F_z(\mathbf{r})$ was used by Schechter and Mozer in computing wave-

TABLE IV. Hyperfine interaction of the S^+ donor electron with Si^{29}.

Symmetry of site	Likely site: Substitutional model	Likely site: Interstitial model	Units of 10^{-4} cm^{-1}: T_1	T_2	T_3	T_I	β (deg.)
111	111	111	−18.9	−6.9	−6.9	−10.9	
	333	222	−3.41	−2.85	−2.85	−3.0	
	444	222	−0.99	−0.97	−0.97	−0.98	
	444	333	−0.52	−0.42	−0.42	−0.45	
100	400	200	−0.71	−0.70	−0.64	−0.68	
110			−3.20	−2.86	−2.62	−2.89	50±3
			−1.61	−1.55	−1.61	−1.59	70±3
			−1.56	−1.19	−1.10	−1.28	55±3

function amplitudes, which Feher then compared with his experimental values. For $F_z(\mathbf{r})$, Schechter and Mozer took[16]

$$F_z(\mathbf{r})=F(r)_{\text{isotr}}\left(\frac{a^{*3}}{a^2b}\right)^{1/2}\times\exp\left[-\left(\frac{x^2+y^2}{n^2a^2}+\frac{z^2}{n^2b^2}\right)^{1/2}\right]\Big/\exp\left(-\frac{r}{na^*}\right). \quad (13)$$

Here $F(r)_{\text{isotr}}$ is an envelope function obtained by solving an isotropic effective-mass equation using the observed binding energy, while the remainder of the expression is an anisotropy correction.

The square of the wave-function amplitude at the lattice site n is given by[16]

$$|\Psi(\mathbf{r}_n)|^2=\tfrac{3}{2}\eta[F_x(r_n)\cos k_0x_n+F_y(r_n)\cos k_0y+F_z(r_n)\cos k_0z_n]^2, \quad (14)$$

where η is defined as

$$\eta=u(\mathbf{r}_n)^2/\langle u(\mathbf{r})\rangle^2, \quad (15)$$

and the average is taken over the unit cell.

The above procedure for calculating $|\Psi(\mathbf{r}_n)|^2$ can easily be adapted to S^+. The major difference from the shallow donor case arises from the fact that the core of the S^+ ion is doubly rather than singly charged. As an approximation to the impurity potential we therefore take $U_s(\mathbf{r})=-Ze^2/\kappa r$, substitute (11) into (10) and find $a_s=a/Z$, $b_s=b/Z$, and $(E_{\text{eff mass}})_s=Z^2E_{\text{eff mass}}$, where $Z=2$ for S^+. Using 0.52 eV for the ionization energy of S^+,[17,18] the mean effective radius of the donor orbital $n_sa_s^*=4.75$ Å, as compared to the value 16.9 Å for phosphorus. This radius, however, remains larger than distances to near neighbors, and one still expects interference effects to be important in (14). Theoretical values of $|\Psi(r_n)|^2$ were obtained from Eqs. (12)–(15) using $(E_{\text{obs}})_s=0.52$ eV, $k_0=0.85k_{\max}$, $a_s=12.5\times10^{-8}$ cm, $b_s=7.1\times10^{-8}$ cm, $\eta=186$, and $F(r_n)_{\text{isotr}}=(\pi n_s^3a_s^{*3})^{-1/2}\exp[-(r_n/n_sa_s^*)]$. In Table V, we give calculated values of the contact part of the hyperfine interaction, obtained from $|\Psi(r_n)|^2$ and (6).

Some of the approximations used in arriving at our calculated values of the contact interaction are the following: (a) The effective-mass approximation has been used. (b) Contributions of bands other than Δ_1 to the wave function have been ignored. Kohn has estimated[1] that the coefficients α_n describing contributions from other bands will be of order $(E_{\text{obs}}/\Delta E)(a/a^*)\alpha$, ΔE being the band gap energy and a the lattice parameter. For S^+ we find $\alpha_n/\alpha\sim0.1$ for a ΔE of 1 eV. (c) $F(r)_{\text{isotr}}$ was set equal to $(\pi n_sa_s^{*3})^{-1/2}\exp[-r/n_sa_s^*]$. An alternative procedure is to break the space surrounding the impurity ion into inner and outer regions and match solutions at the boundary[1]; however, a problem of normalization is thereby introduced. Ham has kindly examined the solution for the outer region, obtained in terms of Whittaker functions, and finds that it gives an enhancement of the calculated hyperfine interaction with near neighbors over more distant neighbors. For example, the ratio of T for 111 and 400 neighbors is increased by a factor of 2 or 3 beyond that given by Table V. We conclude that values of T in Table V are of doubtful accuracy, but will serve the purpose of the present paper.

TABLE V. Calculated isotropic part of the hyperfine interaction.

Symmetry of site	Substitutional model Site	T (10^{-4} cm^{-1})	Interstitial model Site	T (10^{-4} cm^{-1})
111	111	−2.6	111	−2.6
	333	−2.6	$(222)_a$	−13.4
	$(444)_a$	−1.9	$(222)_b$	−13.4
	$(444)_b$	−1.9	333	−2.6
100	400	−11.9	200	−11.1
	800		600	−3.6
110	220	−0.5		
	311	−0.7	311	−0.7
	331	−0.8	331	−0.8
	$(422)_a$	−2.1	422	−2.1
	$(422)_b$	−2.1	511	−0.8

D. Discussion

Parameters describing the hyperfine interaction of the S^+ donor electron with Si^{29} for eight sets of sites are given in Table IV. As indicated in Sec. IV.A(b), a careful but unsuccessful search for additional large interactions ($T_j>0.42\times10^{-4}$ cm^{-1}) was made, and it is felt that none have been missed. Four of the sets of sites have 111 symmetry. One of these shows by far the largest anisotropic contribution to the hyperfine interaction as well as the largest isotropic interaction. The large anisotropy makes it appear likely that this interaction is with Si^{29} occupying the nearest-neighbor positions.

For axial symmetry, the isotropic part T_I of the hyperfine interaction is defined as $T_I=(T_{II}+2T_\perp)/3$, which generalizes to

$$T_I=(T_1+T_2+T_3)/3 \quad (16)$$

in lower symmetry. We assume the dipolar contribution to T_I to be small, and compare experimental values of it, given in Table IV, with calculated values of the contact interaction given in Table V. Providing the site assignments of Table IV are correct, the interaction with the nearest neighbors is considerably stronger,

[16] This work was described by Feher in Ref. 2.

[17] The value 0.52 eV for the ionization energy of S^+ was obtained by Kravitz and Paul (Ref. 18), who exposed a sample containing S^+ to infrared radiation. They found a marked decrease in the resonance signal for photon energies equal to or greater than 0.52 eV and attributed it to excitation of the donor electron of S^+ from the ground state to the conduction band. Kravitz assigns the 0.37-eV energy level reported in Ref. 7 to the sulfur pairs discussed in Sec. V.A.

[18] L. C. Kravitz and W. Paul (to be published).

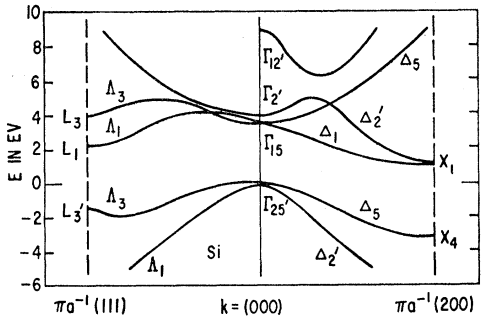

FIG. 8. Sketch of the energy bands of silicon along the [110] and [111] axes of the Brillouin zone. [Adapted from Fig. 6 of J. C. Phillips, Phys. Rev. **125**, 1931 (1962).]

relative to other interactions, than predicted by Table V. Of particular interest is a comparison of the strength of this interaction with that of the nearest neighbors in the cubic directions (the 400 or 200 neighbors, depending upon whether S^+ be substitutional or interstitial). The experimental result is that the interaction is relatively quite strong (-11 as compared to -0.7, in units of 10^{-4} cm^{-1}), while on the basis of the Kohn-Luttinger analysis the interaction with 111 neighbors is expected to be weaker or at most comparable in strength. We thus have a strong disagreement between experiment and the theory.

Ham has considered the possibility that an important source of error is the neglect of contributions of bands other than Δ_1 to the wave function of the donor electron. He points out that the $\Delta_{2'}$ band is the next closest in energy to the S^+ donor level (see Fig. 8). In addition, it alone of the $\Delta_{2'}$, Δ_5, and $\Delta_{5'}$ bands has the proper symmetry to couple with the symmetrical ground state of the donor electron. The Δ_1 and $\Delta_{2'}$ bands are identical under the symmetry operations about a lattice site but behave oppositely under the operation of inversion through the midpoint between two adjacent atoms. Ham anticipates strong coupling between these bands via the impurity potential associated with the S^+ ion. More distant parts of the band structure which on symmetry can contribute are the L_1 and $\Gamma_{2'}$ extrema in the conduction band.

Ham points out that if one assumes contributions to the wave function from both Δ_1 and $\Delta_{2'}$ bands, the contributions which have s character relative to the lattice sites will have opposite relative signs at alternate sites. Presumably, the $\Delta_{2'}$ contribution acts to increase the wave-function amplitude at all sites described by odd integers (e.g., 111 sites) and to decrease it at all sites described by even integers (e.g., 400 and 440 sites), although interference effects may complicate this result. Such an assumption would help to account for the small hyperfine interaction at the 400 sites (assuming S^+ to be substitutional) compared with that at the 111 sites. No quantitative estimate has been made of the effects of $\Delta_{2'}$ admixture upon the hyperfine interaction.

We have not succeeded in producing a strong argument, based on the hyperfine interaction, for deciding whether the S^+ ion is substitutional or interstitial. The assumption that it is substitutional remains perhaps more attractive since sulfur is a double donor as predicted by that model.[7]

Assuming the S^+ ion to be substitutional, we may compare its hyperfine interaction with Si^{29} with that of the shallow donors phosphorus and arsenic, as measured by Feher.[2] For these impurities Feher finds interactions of 111 symmetry, the isotropic part of which ranges from -0.27 to -0.68, in units of 10^{-4} cm^{-1}; he assigns the interactions to Si^{29} occupying 111, 333, and 555 sites.[19] For S^+ the interaction with such neighbors (ignoring ambiguities in assignment) ranges from -0.45 to -10.3 in the same units (see Table IV); the deep donor S^+ shows a greater concentration of wave function in the immediate vicinity of the impurity nucleus. The shallow donors show their largest hyperfine interaction ($\sim -1\times10^{-4}$ cm^{-1}) with Si^{29} occupying the 400 position; for S^+ this interaction is comparatively small (-0.7×10^{-4} cm^{-1}). Interference effects are less pronounced in the case of S^+.

We conclude that the Kohn-Luttinger treatment in its simple form (intended for application to shallow donors) fails to account for the wave-function amplitude at nearby lattice sites of the donor electron of S^+. Ham has suggested that the $\Delta_{2'}$ band may make an important contribution to the wave function.

V. OTHER CENTERS

In the course of our study of sulfur in silicon, sulfur was introduced into crystals containing various concentrations of donor or acceptor impurities and the samples were examined for paramagnetic resonance absorption. Spectra were observed for a number of resonant centers in addition to S^+. One of the centers involves a pair of equivalent sulfur ions, while three others are sulfur-iron pairs. Results on these centers are described in V. The sulfur pairs are of interest in part because they may account for uncertainty which has arisen as to the electrical and optical properties of sulfur in silicon. We now turn to consideration of individual centers.

A. Sulfur Pairs

A spectrum which we attribute to sulfur pairs has been detected in almost every sulfur-doped sample containing fewer than 3×10^{16} acceptors/cm^3. In particular, it was present in samples examined by Carlson *et al.* by electrical techniques in which they found the 0.37-eV electrical level, and in samples

[19] In making this assignment Feher apparently has not taken into consideration the presence of two nonequivalent sets of 444 sites.

studied optically by Krag and Zeiger.[20] The spectrum is shown in Fig. 9 for a sample enriched to 26% in the isotope S^{33}. It consists of a strong line at $g=2.0008$ plus satellite structure. Since the structure is present only in samples enriched in S^{33}, it is clear that the resonant center involves sulfur. However, the intensity of the four stronger satellites relative to that of the main line indicates that they arise from a center containing two equivalent sulfur ions.

The spin Hamiltonian describing a S^{33}–S^{32} center is

$$\mathcal{H}=\beta\mathbf{S}\cdot g\cdot\mathbf{H}+\mathbf{S}\cdot A\cdot\mathbf{I}-\gamma\beta_N\mathbf{H}\cdot\mathbf{I} \qquad (17)$$

with $g=2.0008\pm0.0001$ and $|A|=38.4\times10^{-4}$ cm^{-1}. (A center involving two sulfur ions must have lower than tetrahedral symmetry; however, we have not succeeded in detecting asymmetry in either the g tensor or the hyperfine interaction tensors.[21]) In the case of S^{33}–S^{33} centers, one has

$$\mathcal{H}=\beta\mathbf{S}\cdot g\cdot\mathbf{H}+\sum_{k=1}^{2}(\mathbf{S}\cdot A\cdot\mathbf{I}_k-\gamma\beta_N\mathbf{H}\cdot\mathbf{I}_k). \qquad (18)$$

The spectrum consists of seven hyperfine components, corresponding to the seven values of $m=m_1+m_2$, of relative intensity 1:2:3:4:3:2:1, which account for the weak satellites of Fig. 9.

A search was made for fine structure both in unstrained and in purposely strained crystals. The lack of success is an indication that $S=\frac{1}{2}$. An unsuccessful search was made for ENDOR transitions of S^{33} (analysis of such transitions would lead to a value of the electron spin).

The $g\simeq2$ of the sulfur pair is evidence that the center has no orbital degeneracy in the ground state. If, as seems likely, the center contains an odd number of

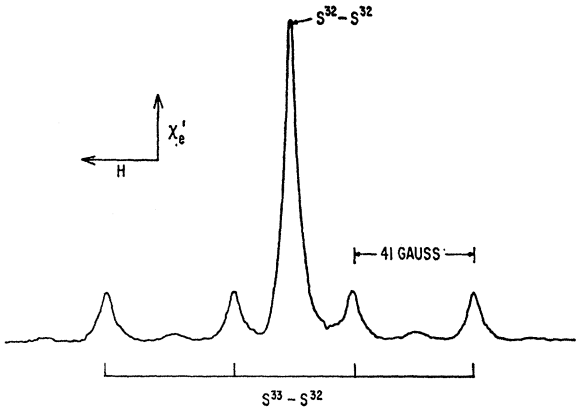

FIG. 9. Spectrum of sulfur pairs under rapid passage conditions in a sample enriched to 26% in the isotope S^{33} ($I=\frac{3}{2}$). The four satellites whose intensity is about 15% that of the main line are attributed to S^{32}–S^{33} pairs. Flanking the outermost of these are still weaker lines which we attribute to S^{33}–S^{33} pairs.

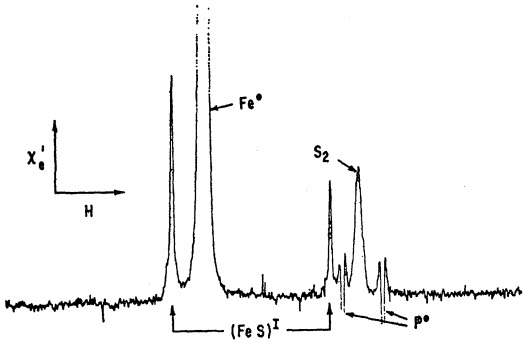

FIG. 10. The spectrum of the $(FeS)^I$ center for H in a [001] direction, where it consists of two lines representing 8 and 4 types of sites, respectively.

electrons ($S=\frac{1}{2}$), the charge state of the center probably is S_2^+. However, no detailed model of the center has been developed.

Kravitz and Paul have reported experiments in which the intensity of the spectrum attributed here to sulfur pairs was monitored while the sample was irradiated with infrared.[18] For $h\nu\gtrsim0.37$ eV, they find a decrease in intensity, coupled, in some samples, with an increase in photoconductivity. They conclude that the 0.37-eV electrical level is associated with sulfur pairs rather than being the second-donor level of isolated sulfur as reported earlier.[7]

B. Iron-Sulfur Pairs

It was difficult to avoid iron contamination in samples prepared to contain sulfur. (The iron was easily recognized by its characteristic paramagnetic resonance spectra.[5]) Additional spectra, which we attribute to iron-sulfur pairs, were found in a number of samples containing sulfur, iron, and either a shallow donor, a shallow acceptor, or no other intentionally added impurities. These spectra are the subject of Sec. V.B.

The spectrum shown in Fig. 10 was found in a number of samples containing phosphorus, sulfur, and iron. It was not detected in samples lacking any one of these impurities. For H in a low symmetry direction in the (110) plane the spectrum consists of seven lines of approximate relative intensity 1:1:2:2:2:2:2. Our interpretation is that the spin Hamiltonian of any one center has the form

$$\mathcal{H}=\beta\mathbf{S}\cdot g\cdot\mathbf{H} \qquad (19)$$

with the principal axes of the g tensor being a [110] direction and two mutually perpendicular directions in the (110) plane (see Fig. 3 with g_1 replacing T_1, etc.). Any one center yields one resonance line. The total spectrum arises from twelve types of sites, each type having a different set of principal axes. Since no fine structure is present, it would appear that $S=\frac{1}{2}$.

The form of the g tensor indicates that the resonant center has reflection symmetry in the (110) plane, but

[20] W. E. Krag and H. J. Zeiger, Phys. Rev. Letters 8, 485 (1962); W. E. Krag (unpublished work).

[21] See, however, the discussion of Sec. V.C.

TABLE VI. Resonance parameters of centers in sulfur-doped silicon at 10°K.

Center	S	g tensor	β (deg.)	hf interaction with Fe^{57} (10^{-4} cm^{-1})
$(FeS)^{I}$	$\frac{1}{2}$	$g_1=2.046$	15 ± 2	$\lvert A_1\rvert<2$
		$g_2=2.010$		$\lvert A_2\rvert\sim 2.2$
		$g_3=2.126$		$\lvert A_3\rvert=5.8$
$(FeS)^{II}$	$\frac{1}{2}$	$g_1=2.962$	28.5± 2	$\lvert A_1\rvert<3$
		$g_2=1.938$		$\lvert A_2\rvert=9.3$
		$g_3=2.015$		$\lvert A_3\rvert=4.7$
$(FeS)^{III}$	$\frac{1}{2}$	$g_1=2.503$	46.0± 1	
		$g_2=1.991$		
		$g_3=2.042$		
U	$\frac{1}{2}$	$g_1=1.997$	≈ 90	
		$g_2=2.002$		
		$g_3=2.001$		

otherwise has low symmetry. The center cannot be an isolated sulfur ion at a site of tetrahedral symmetry but rather would appear to be a sulfur ion paired with another impurity ion, such as iron.[22] This surmise was confirmed by intentionally introducing both Fe^{57} and sulfur into phosphorus-doped silicon. For some directions of magnetic field, Fe^{57} hyperfine structure could then be observed and studied. Unfortunately, it was not possible to obtain a supply of sulfur enriched in S^{33} to use in searching for S^{33} hyperfine structure. Thus the only evidence that the center involves sulfur is that it has been detected only in samples known to contain sulfur.

A spectrum having the same symmetry but different resonance parameters was observed in crystals containing sulfur and iron but no other intentionally added impurities. Fe^{57} hyperfine structure was observed in samples prepared to contain iron enriched in that isotope.

A third spectrum of the same symmetry was found in crystals containing sulfur, iron, and boron. In this case, both Fe^{57} and S^{33} hyperfine structure were detected, but were not studied in detail.

The centers observed using phosphorus-doped, undoped, and boron-doped silicon starting material are designated the $(FeS)^{I}$, $(FeS)^{II}$, and $(FeS)^{III}$ centers, respectively. Their resonance parameters are summarized in Table VI. The data is incomplete in that the principal axes of the tensor describing the hyperfine interaction with Fe^{57} were not located. Thus the values for that interaction given in Table VI are not necessarily principal values, but rather pertain to the directions which are principal axes of the g tensor.

From the symmetry of the g tensor it would appear that each center consists of an iron ion and a sulfur ion lying in a (110) plane. One possibility is that in forming the centers an interstitial iron ion diffuses to a site occupied by a sulfur ion, and in the resulting complex the two ions lie along a low symmetry direction in a (110) plane, perhaps jointly occupying one substitutional site. Each center apparently is described by electron spin $\frac{1}{2}$. It is quite possible that the $(FeS)^{I}$ and $(FeS)^{III}$ spectra are associated with the singly negatively and singly positively charged states of the same complex.

Electrical properties of the pairs have not been studied and might well be difficult to unravel.

The iron-sulfur pairs of present concern do not appear to be analogous to pairs formed by iron with acceptor impurities such as boron, gallium, and indium.[5] The latter pairs have higher symmetry and are of the donor-acceptor type.

C. Unidentified Center

In samples doped with sulfur of normal isotopic abundance, the spectrum of sulfur pairs consists of one line at $g=2.0008$. However, in many samples some anisotropy has been detected in this absorption. It is felt that probably a second, slightly anisotropic spectrum (labeled U) is present, although the possibility that one is simply detecting the anisotropy of the sulfur pair spectrum has not been completely ruled out.[23] The spectrum is difficult to analyze because the anisotropy is relatively small. However, it appears that the symmetry of the g tensor is the same as for the iron-sulfur pairs described in Sec. V.B or perhaps higher (100 symmetry). Tentative values of resonance parameters are given in Table VI.

ACKNOWLEDGMENTS

The author wishes to thank the following for their contributions to this work: F. S. Ham, for considering the possibility that bands other than Δ_1 might contribute to the wave function of the S^+ donor electron and suggesting the importance of the $\Delta_{2'}$ band, and also for additional discussions; H. H. Woodbury, for participating in early experiments; R. O. Carlson for discussions; C. R. Trzaskos, for experimental assistance; R. O. Carlson and G. D. Brower, for preparing a number of early samples and furnishing data on their electrical characteristics; W. E. Krag, for sending samples of sulfur-doped silicon and informal discussions; and L. C. Kravitz and W. Paul, for communicating results of their combined infrared-paramagnetic resonance experiments prior to publication.

[22] Another common impurity in silicon crystals is oxygen. However, the spectrum here described has similar intensities in crystals of low oxygen content (floating zone silicon) and in crystals of high oxygen content (quartz-crucible grown silicon).

[23] Were S^{33} available, it should be relatively simple to check whether the U center is or is not distinct from the sulfur-pair center.